

# A Practical Guide to First-Order Multiplet Analysis in $^1\text{H}$ NMR Spectroscopy

Thomas R. Hoye,\* Paul R. Hanson,<sup>1a</sup> and James R. Vyvyan<sup>1b</sup>

Department of Chemistry, University of Minnesota, Minneapolis, Minnesota 55455

Received March 9, 1994<sup>o</sup>

The ability to deduce the proper set of coupling constant ( $J$ ) values from a complex first-order multiplet in a  $^1\text{H}$  NMR spectrum is an extremely important asset. This is particularly valuable to the task of assigning relative configurations among two or more stereocenters in a molecule. Most books and treatises that deal with coupling constant analysis address the less useful operation of generating splitting trees to create the line pattern from a given set of  $J$  values. Presented here are general and systematic protocols for the converse, i.e., for deducing the complete set of  $J$  values from the multiplet. Two analytical methods (A, systematic analysis of line spacings, and B, construction of what can be called inverted splitting trees) are presented first. A reasonably thorough and systematic set of graphical representations of common doublet of doublets (dd's), ddd's, and dddd's are then presented. These constitute a complementary method for identification of  $J$ 's through visual pattern recognition. These approaches are effective strategies for extraction of coupling constant values from even the most complex first-order multiplets.

## Introduction

Proton NMR spectroscopy is, arguably, the most powerful tool for structure assignment in most classes of organic molecules. Increased access to spectral data acquired on higher-field NMR spectrometers means that more and more of the resonances in routine spectra are first-order. While it is true that most modern spectrometers (as well as an increasing number of desktop personal computers) have software routines capable of performing rapid simulation of multispin systems, this approach to the analysis of complex first-order multiplets is often cumbersome, time consuming, or less than convenient. Simulation of a given multiplet is largely an empirical process that requires an initial determination or estimate of several of the individual coupling constants. Thus, the use of these computer-aided algorithms for the generation of simple first-order multiplets is less attractive than the ability to deduce a correct set of coupling constants upon simple visual inspection of any of the typically encountered line patterns. Graphical representations of common multiplet patterns are, in principle, quite useful for comparative analysis of actual data, but nearly all the published work has focused on non-first-order multiplets.<sup>2</sup> The general application of such representations is somewhat limited for two reasons: second-order multiplets are less frequently encountered at higher fields, and if one's spin system does not have the precise  $\Delta\nu/J$  value of the calculated spectrum, the multiplet in question may look significantly different from the published representation.

The emergence of routine multidimensional NMR spectroscopy has been accompanied by a decline in the learning, teaching, and practice of the important skill of assigning first-order multiplets by inspection. Determination of coupling constants is still the most valuable

general method for assigning relative configurations of stereogenic centers in molecules. While the power of various routine two-dimensional NMR experiments is unarguable, it comes with a price. Data collection for 2-D experiments is always more time-consuming than for the simpler 1-D experiment, and in most settings access to magnet time is finite. Since 1-D and 2-D methods often provide complementary structural information, it is important that chemists maintain expertise with both.

This paper describes two related methods (A and B) that allow one to identify individual coupling constants within even the most complex first-order multiplets likely to be encountered in  $^1\text{H}$  NMR spectra. It also provides a set of graphical representations (C and Tables 1-11) for assisting in empirical, visual pattern recognition.

A first-order multiplet arises when no two of the spins within an interacting multispin system have  $\delta\nu/J \leq \sim 6$ , and it always contains a symmetrical distribution of line positions about the midpoint of the multiplet (i.e., the chemical shift).<sup>3</sup> In first-order multiplets the distance between the outermost pair of peaks is the sum of each of the coupling constants ( $\Sigma J$ 's), a fact that we frequently find useful in assigning or verifying, for example, the last  $J$  value for an incompletely resolved complex multiplet.<sup>4</sup> Often "special relationships" exist among the sets of coupling constants. We define these as cases where one of the coupling constants is equal to some combination of sums and/or differences among the remaining coupling constants. So defined, these special relationships always serve to reduce the number of lines in the multiplet and simplify (or complicate, depending on one's experience and point of view) the observed pattern. Finally, note that it is often, but by no means always, possible to determine a given coupling constant from either of a pair of spin-coupled resonances.

## Methods for Deducing Coupling Constant Values

### A. Systematic Analysis of Line Spacings. The task of extracting the actual values of coupling constants

(3) Caution must be exercised, however, because many second-order patterns (e.g., AB, AA'BB', AA'XX', and ABX) are also symmetrical.

(4) Often the sum of the  $J$ 's for non-first-order multiplets is also the distance between the outside lines of the multiplet, but this relationship deteriorates by the appearance of additional lines as  $\Delta\nu/J$  becomes smaller and smaller.

\* Abstract published in *Advance ACS Abstracts*, June 15, 1994.

(1) (a) University of Minnesota Graduate School Fellow, 1991-92. (b) Hercules Fellow, 1993-94.

(2) (a) Jackman, L. M., Sternhell, S. In *International Series of Monographs in Organic Chemistry*; Barton, D. H. R., Doering, W., Eds.; Oxford: Pergamon Press, 1969; Vol. 5: Applications of Nuclear Magnetic Resonance Spectroscopy in Organic Chemistry, Chapters 2 and 4 and references therein. (b) Wiberg, K. B., Nist, B. J. *The Interpretation of NMR Spectra*; W. A. Benjamin: New York, 1962. (c) Becker, E. D. *High Resolution NMR: Theory and Chemical Applications*, Academic Press: New York, 1980 and references therein.

Chart 1. Association between Coupling Constants and Line Spacings<sup>a</sup> within dd's and ddd's

	Association	Line Spacing	Description
for dd's	$J_L$	{1 to 3} <sup>a</sup> (= {2 to 4})	larger J
	$J_S$	{1 to 2} (= {3 to 4})	smaller J
	$\Sigma J's = J_L + J_S$	{1 to 4}	sum of J's
	$J_L - J_S$	{2 to 3}	difference of J's
for ddd's	$J_L$	{1 to 5} (= {2 to 6} = {3 to 7} = {4 to 8})	largest J
where	$J_M$	{1 to 3} (= {2 to 4} = {5 to 7} = {6 to 8})	medium J
$J_L \geq J_M + J_S$	$J_S$	{1 to 2} (= {3 to 4} = {5 to 6} = {7 to 8})	smallest J
	$\Sigma J's = J_L + J_M + J_S$	{1 to 8}	sum of J's
	$J_M + J_S$	{1 to 4} (= {5 to 8})	sum of smaller two J's
	$J_M - J_S$	{2 to 3} (= {6 to 7})	difference of smaller two J's
	$J_L + J_M$	{1 to 7} (= {2 to 8})	sum of larger two J's
	$J_L - J_M$	{3 to 5} (= {4 to 6})	difference of larger two J's
	$J_L + J_S$	{1 to 6} (= {3 to 8})	sum of largest and smallest J's
	$J_L - J_S$	{2 to 5} (= {4 to 7})	difference of largest and smallest J's
for ddd's	$J_L$	{1 to 4} (= {2 to 6} = {3 to 7} = {5 to 8})	largest J
where	$J_M$	{1 to 3} (= {2 to 5} = {4 to 7} = {6 to 8})	medium J
$J_L \leq J_M + J_S$	$J_S$	{1 to 2} (= {3 to 5} = {4 to 6} = {7 to 8})	smallest J
	$\Sigma J's = J_L + J_M + J_S$	{1 to 8}	sum of J's
	$J_M + J_S$	{1 to 5} (= {4 to 8})	sum of smaller two J's
	$J_M - J_S$	{2 to 3} (= {6 to 7})	difference of smaller two J's
	$J_L + J_M$	{1 to 7} (= {2 to 8})	sum of larger two J's
	$J_L - J_M$	{3 to 4} (= {5 to 6})	difference of larger two J's
	$J_L + J_S$	{1 to 6} (= {3 to 8})	sum of largest and smallest J's
	$J_L - J_S$	{2 to 4} (= {5 to 7})	difference of largest and smallest J's

<sup>a</sup> {i to j} = the separation in hertz between lines i and j.

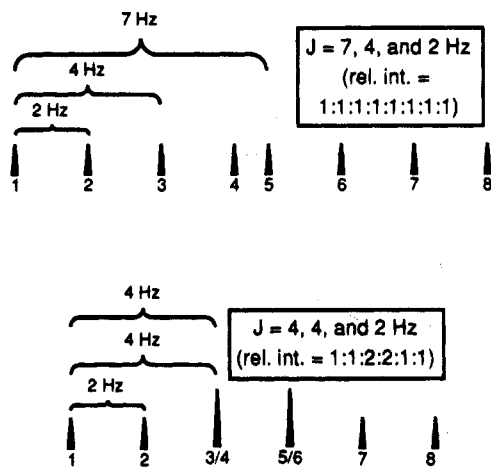


Figure 1. Examples of ddd's where  $J_L \geq J_M + J_S$  (case i) and where  $J_L \leq J_M + J_S$  (case ii).

from within a given multiplet is most obvious for simple doublet of doublets (dd's). If the lines of the multiplet are numbered sequentially from, say, left to right (cf. entry a in Table 1), two (of the six) pairs of line spacings are associated with the smaller  $J$  value. As also summarized in the top portion of Chart 1, two more pairs of line spacings are associated with the larger  $J$ , and the remaining two pairs represent, respectively, the sum of and difference between the large and small  $J$ 's. The

distance between lines  $i$  and  $j$  is denoted as { $i$  to  $j$ } throughout the discussion.

It is important to recognize that even though various sets of lines can have the same spacing, not all of those sets represent a coupling constant; some are coincidental. This is often a point of confusion. For example the distances between lines 1 to 2, 2 to 3, and 3 to 4 in entry b in Table 1 are all identical even though only {1 to 2} and {3 to 4} represent an actual  $J$ ; {2 to 3} is the difference between the two  $J$ 's (and {1 to 4} is the sum of the two  $J$ 's).

The situation for doublet of doublet of doublets (ddd's, bottom portion of Chart 1) is somewhat more complex, but still readily decipherable. For this treatment it is useful to define the  $J$ 's as  $J_s$ ,  $J_m$ , and  $J_l$  to correspond to the smallest, medium, and largest  $J$ 's of the ddd, respectively. Again, the lines are numbered sequentially from left to right. The relative line intensities are important. In the absence of special relationships, all lines are of equal intensity, and for a ddd there is a total of eight lines [cf. the example in case i) in Figure 1]. One frequently encounters multiplets that contain line superposition, which is always accompanied by differential relative line intensities and a reduction in the total number of lines [cf. the example in case ii) in Figure 1]. Under any circumstances the sum of the relative line intensities will always equal 8 for a ddd (4 for a dd, 16 for a dddd, etc.). Lines of relative intensity greater than one are assigned more than one line number [e.g., the

sequence 1-(2/3/4)-(5/6/7)-8 for a 1:3:3:1 apparent quartet (ddd with three equivalent  $J$ 's) or the example in case ii)]. Be aware that "leaning" within a given multiplet, arising from intermediate  $\Delta\nu/J$  values for which first-orderedness still holds, will distort the relative intensities from perfect integer ratios.

For doublet of doublet of doublets two situations can arise: case i where  $J_1 \geq J_m + J_s$  and case ii where  $J_1 \leq J_m + J_s$ . A typical example for each case is shown in Figure 1.<sup>5</sup> With the lines now numbered as described above and with reference to the bottom portion of Chart 1, one can assign the values of  $J_s$ ,  $J_m$ , and  $J_1$  in each of these multiplets by measuring the appropriate line spacings. The distance between lines 1 and 2 (i.e., {1 to 2}) always corresponds to the smallest coupling constant ( $J_s$ ) and {1 to 3} always corresponds to the next smallest coupling constant ( $J_m$ ). However,  $J_1$  corresponds to {1 to 5} for case i but to {1 to 4} for case ii. The task of identifying  $J_1$  from within dddd's (or higher multiplets) by this strategy is considerably more difficult. However, removing the smallest coupling ( $J_s$ ) from a dddd, thereby creating a simplified ddd, permits application of the above strategy. On the other hand, this simplification is the first step in creating what we call here an inverted splitting tree, a process that is generalized next.

**B. Inverted Splitting Tree Generation.** The process of deconvoluting a first-order multiplet more complex than a ddd by the method described in A is not straightforward. We now describe a systematic approach that is applicable to even the most complex first-order multiplets. This strategy amounts to generation of an inverted splitting tree. Many readers are familiar with the process of generating the appearance of a first-order multiplet from a given set of  $J$  values, and many texts present the creation of splitting trees from a single line by sequential branching (most easily done proceeding from the largest  $J$  to the smallest). However, the ability to do the converse, to deduce the proper individual  $J$ 's from a given complex multiplet, is the more valuable yet more difficult skill to attain.

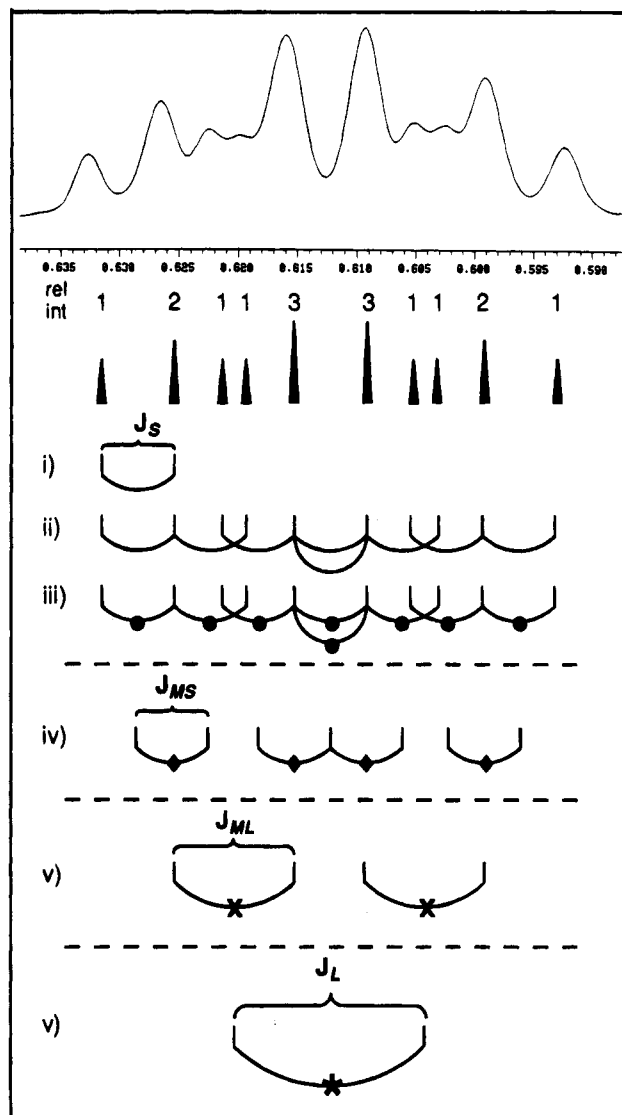
The total number of lines and the relative line intensities within a given multiplet are important parameters. Recall that dd's, ddd's, and dddd's with no special relationships will consist of 4, 8, and 16 lines, respectively, all of equivalent intensity and that the presence of special relationships among the coupling constants both reduces the total number of lines and alters the relative line intensities. The sum of the line intensities, appropriately normalized, will be identical for every multiplet of a given class (i.e., 4 for dd's, 8 for ddd's, and 16 for dddd's).

A general protocol for deducing the individual  $J$ 's for a given multiplet (illustrated in Chart 2 specifically for the ten-line 1:2:1:1:3:3:1:1:2:1 dddd corresponding to entry e of Table 9) consists of the following:

Step i: As discussed earlier, the distance between lines 1 and 2 (or the, say, left-hand-most pair) always represents the smallest  $J$  value of the multiplet [cf.,  $J_s$  in panel i) of Chart 2]. If their relative intensity is 1:1, then the smallest  $J$  is unique; if it is 1:2 (or 1:3, etc.), then there are two (or three, etc.) identical smallest  $J$ 's.

Step ii: Identify the full set of pairs of lines separated by this smallest  $J$  value. This is perhaps the most diffi-

**Chart 2. Protocol for Generating an Inverted Splitting Tree: Identification of Individual Coupling Constants as Applied to the dddd from Entry e of Table 9**



cult step in the process. A dddd will contain eight such pairs. Each pair will have a partner pair symmetrically arranged by reflection through the midpoint of the multiplet. Those pairs associated with lines of intensities  $> 1$  will be partially or totally coincident with other pairs. Thus, the total number of pairs associated with any single line is equal to the relative intensity of that line. As seen in panel ii), this is manifested in the number of times the ends of interconnecting arcs intersect a given line position (or vertical tick). That is, lines of intensities 1, 2, and 3 in the multiplet in Chart 2 have the ends of one, two, or three arcs, respectively, terminating at that line position [cf. panel ii)].

Step iii: Identify the centers of each of the pairs created in step ii, which collectively represent a new, simplified pattern (a ddd) as indicated by the dots in panel iii) as well as the tick marks in panel iv) in Chart 2. Notice that this submultiplet (in this instance a seven-line 1:1:1:2:1:1:1 ddd) is the residual pattern that would remain after selective decoupling of the spin responsible for the smallest  $J$  in the original multiplet. The spacing between the first (or last) pair of dots in this simplified multiplet represents the next smallest  $J$  of the original

(5) Notice that the examples chosen to illustrate cases i and ii were somewhat arbitrarily chosen. Examples could easily have been selected in which the case i and case ii multiplets contained fewer than and exactly eight total lines, respectively, rather than the converse.

Table 1. dd's

entry	Multiplet Appearance	$J_x$ $J_{13}$	$J_y$ $J_{12}$	$\Sigma$ $J$ 's	Special Relationships
a		12	4	16	
b		8	4	12	
c		6	4	10	
d		5	4	9	
e		4	4	8	$J_{13} = J_{12}$
f		3	4	7	
g		2	4	6	
h		1	4	5	
i		0	4	4	

$\text{H}$   $\delta = 0.61$ ; dd;  $J = 8.3, 3.8$  Hz; entry b  
 $\text{H}$   $\delta = 0.44$ ; dd;  $J = 3.8, 3.8$  Hz; entry e

Table 2. ddd's Where  $J_y = J_x$  (app dt's)

entry	Multiplet Appearance	$J_x$ $J_{14}$	$J_y = J_x$ $J_{12} = J_{12'}$	$\Sigma$ $J$ 's	Special Relationships
a		20	4=4	28	
b		12	4=4	20	
c		9	4=4	17	
d		8	4=4	16	$J_{14} = J_{12} + J_{12'}$
e		7	4=4	15	
f		6	4=4	14	
g		5	4=4	13	
h		4	4=4	12	$J_{14} = J_{12}$
i		3	4=4	11	
j		2	4=4	10	
k		1	4=4	9	
l		0	4=4	8	

$\text{H}$   $\delta = 3.72$ , ddd,  $J = 11.3, 11.3, 2.5$  Hz  
 entry k

multiplet [i.e.,  $J_{ms(\text{medium small})}$  in panel iv); incidentally note that  $J_s = J_{ms}$  for the example in Chart 2].

Step iv: The centers of each of these new pairs [diamonds in panel iv] collectively represent a new, further simplified, four-line pattern (a dd). The distance between the first (or last) pair of diamonds in panel iv) as well as the tick marks in panel v) represents the third smallest coupling constant,  $J_{ml(\text{medium large})}$ .

Step v: Repeat as necessary until all  $J$ 's have been established. One simple check for internal consistency is to verify that the sum of the determined coupling constants ( $\Sigma J$ 's) is equal to the distance between the two outermost lines of the multiplet.

**C. Graphical Representations (Tables 1–11).** An alternative strategy for analysis of first-order multiplets is through visual pattern recognition. Many will find this approach complementary or preferable to the more analytical methods discussed above. We have generated a series of tables that shows systematic sets of first-order multiplets for the most commonly encountered spin systems. Representations of dd's and ddd's as well as of the more complex doublet of doublet of doublet of doublets (5 spins, dddd's) are included. Within any one table a single coupling constant, arbitrarily named  $J_z$ , is varied from large to small (usually to 0 Hz) values; the remaining coupling constants ( $J_y, J_x, J_w$ ) are invariant throughout any one table. As a consequence, within any one table, entry a consists of relatively widely spaced, identical halves of the multiplet that converge as the variable

$J_z$  decreases until the two halves are superimposed in the limit where the  $J_z = 0$ . Intermediate entries correspond to partially merged situations in which the two halves have undergone one or more sequential crossings of the innermost lines.

For some of the Table entries, special relationships (vide supra) exist among the  $J$ 's. These relationships, along with the magnitudes of  $J_w, J_x, J_y, J_z$ , and the  $\Sigma J$ 's, are listed in the right-hand columns of each table. Note that although a specific (but arbitrary) set of  $J$  values has been chosen for illustrating the trends within any one table, those trends hold, of course, for any set of  $J$ 's having similar relative magnitudes and special relationships.

For any given table the specific line numbers that correspond to the generic  $J_w, J_x, J_y$ , and  $J_z$  are noted below the generic column heading. These line numberings change from table to table. For example,  $J_z$  in Table 1 is  $J_{13}$  (i.e., |1 to 3|) while  $J_z$  in Table 2 is  $J_{14}$ .

Note that the line numberings used in Tables 1–11 do not follow the rigorous convention used in sections A and B. Instead, the multiplet in entry a is simply numbered from left to right disregarding relative line intensities. Thus, each line has a single number at the outset (entry a), the crossing phenomena just mentioned are more easily tracked, identification of  $J$ 's within a visually matched multiplet is facilitated, and, importantly, the line spacings corresponding to every coupling constant, including the variable  $J_z$ , remain the same for all entries in the table.

Table 3. ddd's Where  $J_y \approx J_x$ 

entry	Multiplet Appearance	$J_x$ $J_{12}$	$J_y$ $J_{13}$	$J_z$ $J_{12}$	$\Sigma$ $J$ 's	Special Relationships
a		9	4	3	16	
b		8	4	3	15	
(c)		7	4	3	14	$J_{15} = J_{13} + J_{12}$
d		6	4	3	13	
e		5	4	3	12	
f		4	4	3	11	$J_{15} = J_{13}$
g		3	4	3	10	$J_{15} = J_{12}$
h		2	4	3	9	
i		1	4	3	8	$J_{15} = J_{13} - J_{12}$
l		0	4	3	7	

Table 4. ddd's Where  $J_y = 2J_x$ 

entry	Multiplet Appearance	$J_x$ $J_{12}$	$J_y$ $J_{13}$	$J_z$ $J_{12}$	$\Sigma$ $J$ 's	Special Relationships
a		10	4	2	16	
b		8	4	2	14	
c		7	4	2	13	
(d)		6	4	2	12	$J_{15} = J_{13} + J_{12}$
e		5	4	2	11	
f		4	4	2	10	$J_{15} = J_{13}$
g		3	4	2	9	
h		2	4	2	8	$J_{15} = J_{12}$
i		1	4	2	7	
j		0	4	2	6	

Included in each table is one (or two) representative multiplet(s) arising from the circled (or boxed) proton(s) taken from  $^1\text{H}$  NMR spectra of known molecules.<sup>6</sup> Although many of these presentations are simulations<sup>7</sup> of tabulated  $J$  values (since they are taken from "pre-electronic storage" spectra), we have confirmed that this is an accurate representation of the actual spectrum by simulating multiplets for which the actual spectra were available. The examples in Tables 1, 4, 5, 9(e), and 10 (g) are taken from "real" rather than simulated spectra. The examples in all of the tables were selected to illustrate cases where special relationships exist among the  $J$ 's. These are particularly instructive since first-order multiplets with no special relationships give a full complement of 4, 8, 16, ... lines of identical intensity that are relatively easy to identify and interpret.

Table 1 and Tables 2–5 contain all the possible permutations of relative  $J$  values for dd's and ddd's, respectively. In other words, every conceivable first-order dd and ddd pattern can be approximately matched to one of the entries in these tables. On the other hand, only a somewhat arbitrarily chosen representative set (vide infra) of all possible dddd's is illustrated in Tables 6–11.

Table 1 shows the familiar series of typical doublet of doublets. Notice that there are several relative line

Table 5. ddd's Where  $J_y > J_x$ 

entry	Multiplet Appearance	$J_x$ $J_{12}$	$J_y$ $J_{13}$	$J_z$ $J_{12}$	$\Sigma$ $J$ 's	Special Relationships
(a)		9	6	1	16	
b		8	6	1	15	
(c)		7	6	1	14	$J_{15} = J_{13} + J_{12}$
(d)		6	6	1	13	$J_{15} = J_{13}$
e		5	6	1	12	$J_{15} = J_{13} - J_{12}$
f		4	6	1	11	
g		3	6	1	10	
h		2	6	1	9	
i		1	6	1	8	$J_{15} = J_{12}$
j		0	6	1	7	

(6) Spectral data were collected on a variety of spectrometers ranging from 300 to 500 MHz. (a) Examples from Tables 1, 5, and 9, entry e: Vyvyan, J. R. Unpublished results. (b) Examples from Tables 2, 6, entry f, 7, and 8: North, J. T. Ph. D. Dissertation, University of Minnesota, 1990. (c) Examples from Tables 3, 9, entry g, and 10, entry c: Peck, D. R. Ph. D. Dissertation, University of Minnesota, 1984. (d) Example from Table 4: Koltun, D. O., Vyvyan, J. R. Unpublished results. (e) Examples from Tables 6, entry c, and 11: Dellaria, J. F. Ph. D. Dissertation, University of Minnesota, 1982. (f) Example from Chart 3: Renner, M. K., Priest, O. P. Unpublished results.

(7) Simulation was performed with the VNMR version 4.1 software package on a Varian VXR spectrometer using a spectrometer frequency of 500 MHz and a line width ranging from 0.5 to 0.7 Hz.

spacings that repeat themselves during the progression of  $J_{x(13)}$  from large to small. For example, entries a and h are each a pair of narrowly spaced outer and a pair of widely spaced inner lines. Similarly, entries b and g are

Table 6. dddd's Where  $J_y = J_x = J_w$  (app dq's)

entry	Multiplet Appearance	$J_x$ $J_{12}$	$J_y = J_x = J_w$ $J_{12} = J_{12} = J_{12}$	$\Sigma$ $J$ 's	Special Relationships
a		12	2=2=2	18	
b		8	2=2=2	14	
c		7	2=2=2	13	
d		6	2=2=2	12 $J_{15} = J_{12} + J_{12} + J_{12}$	
e		5	2=2=2	11	
f		4	2=2=2	10 $J_{15} = J_{12} + J_{12}$	
g		3	2=2=2	9	
h		2	2=2=2	8 $J_{15} = J_{12} = J_{12} = J_{12}$	
i		1	2=2=2	7	
j		0	2=2=2	6	

$\delta = 2.23$ , dddd,  $J = 13.9, 4.3, 4.2, 4.0$  Hz  
entry c

BrC1CC2OC(=O)C12

$\delta = 2.03$ , dddd,  $J = 13, 6.5, 6.5, 6.5$  Hz  
entry f

COC1C(Br)CC1

Table 7. dddd's Where  $J_x = J_y$  and  $J_x = J_w$  (app tt's)

entry	Multiplet Appearance	$J_x = J_y$ $J_{14} = J_{14}$	$J_x = J_w$ $J_{12} = J_{12}$	$\Sigma$ $J$ 's	Special Relationships
a		8=8	2=2	20	
b		6=6	2=2	16	
c		5=5	2=2	14	
d		4=4	2=2	12 $J_{14} = J_{12} + J_{12}$	
e		3=3	2=2	10	
f		2=2	2=2	8 $J_{14} = J_{12}$	
g		1=1	2=2	6 $J_{12} = J_{14} + J_{14}$	
h		0=0	2=2	4	

$\delta = 3.95$ , dddd,  $J = 6.2, 6.2, 5.1, 5.1$  Hz  
entry e

CCC(O)C(C)C#N

Table 8. dddd's Where  $J_y = J_x$  (app dtd's)

entry	Multiplet Appearance	$J_x$ $J_{17}$	$J_y = J_x$ $J_{12} = J_{12}$	$J_w$ $J_{12}$	$\Sigma$ $J$ 's	Special Relationships
a		14	4=4	2	24	
b		11	4=4	2	21	
c		10	4=4	2	20 $J_{17} = J_{15} + J_{15} + J_{15}$	
d		9	4=4	2	19	
e		8	4=4	2	18 $J_{17} = J_{15} + J_{15}$	
f		7	4=4	2	17	
g		6	4=4	2	16 $J_{17} = J_{15} + J_{12}$	
h		5	4=4	2	15	
i		4	4=4	2	14 $J_{17} = J_{15} = J_{12}$	
j		3	4=4	2	13	
k		2	4=4	2	12 $J_{17} = J_{12}$	
l		1	4=4	2	11	
m		0	4=4	2	10	

$\delta = 2.80$ , dddd,  $J = 12.0, 3.0, 3.0, 1.0$  Hz  
entry a

C1CC2OC1C2

Table 9. dddd's Where  $J_x = J_w$  (app dtd's)

entry	Multiplet Appearance	$J_x$ $J_{17}$	$J_y$ $J_{12}$	$J_x = J_w$ $J_{12} = J_{12}$	$\Sigma$ $J$ 's	Special Relationships
a		12	5	3=3	23	
b		11	5	3=3	22 $J_{17} = \Sigma J_{12,12,12}$	
c		10	5	3=3	21	
d		9	5	3=3	20	
e		8	5	3=3	19 $J_{17} = J_{15} + J_{12}$	
f		7	5	3=3	18	
g		6	5	3=3	17 $J_{17} = J_{12} + J_{12}$	

$\delta = 0.61$ , dddd,  $J = 8.7, 5.3, 3.4, 3.4$  Hz  
entry e

CCCC1C(=O)C1

$\delta = 1.96$ , dddd,  $J = 14.0, 8.2, 7.0, 7.0$  Hz  
entry g

CC1(C)OC(=O)C1

each a set of four equally spaced lines; they also have the same special relationship. Finally, the number of lines is reduced to three (cf. entry e) in the trivial and common case of a dd appearing as an apparent triplet with relative line intensities of 1:2:1.

Tables 2–5 show the multiplets associated with doublet of doublet of doublets under circumstances where two of the three coupling constants are equal ( $J_{y(12')} = J_{x(12)}$ , Table 2), nearly equal ( $J_{y(13)} \approx J_{x(12)}$ , Table 3), related by a factor of two ( $J_{y(13)} = 2J_{x(12)}$ , Table 4), or very different ( $J_{y(13)} \gg J_{x(12)}$ , Table 5). Table 2 contains the case where the two invariant coupling constants ( $J_{y(12')}$  and  $J_{x(12)}$ ) of

Table 10. dddd's Where  $J_y \approx J_x \approx J_w$ 

entry	Multiplet Appearance	$J_x$ $J_{19}$	$J_y$ $J_{14}$	$J_z$ $J_{13}$	$J_w$ $J_{12}$	$\Sigma$ $J'$ 's	Special Relationships
a		12	5	4	3	24	$J_{19} = \Sigma J_{14, 12, 12}$
b		10	5	4	3	22	
c		9	5	4	3	21	$J_{19} = J_{14} + J_{12}$
d		8	5	4	3	20	$J_{19} = J_{14} + J_{12}$
e		7	5	4	3	19	$J_{19} = J_{12} + J_{12}$
f		6	5	4	3	18	$J_{19} = J_{14} + J_{12} - J_{12}$
g		5	5	4	3	17	$J_{19} = J_{14}$
h		4	5	4	3	16	$J_{19} = J_{12}$
i		3	5	4	3	15	$J_{19} = J_{12}$
j		2	5	4	3	14	$J_{19} = J_{14} - J_{12}$
k		1	5	4	3	13	$J_{19} = J_{12} - J_{12}$
l		0	5	4	3	12	

$\delta = 1.83$ , dddd,  $J = 14.0, 7.6, 6.5, 5.0$  Hz  
entry c

$\delta = 4.23$ , dddd,  $J = 6.5, 6.5, 5.3, 3.8$  Hz  
entry g

Table 11. dddd's Where  $J_y \gg J_x \approx J_w$ 

entry	Multiplet Appearance	$J_x$ $J_{19}$	$J_y$ $J_{15}$	$J_z$ $J_{13}$	$J_w$ $J_{12}$	$\Sigma$ $J'$ 's	Special Relationships
a		12	7	3	2	24	$J_{19} = J_{15} + J_{13} + J_{12}$
b		11	7	3	2	23	
c		10	7	3	2	22	$J_{19} = J_{15} + J_{12}$
d		9	7	3	2	21	$J_{19} = J_{15} + J_{12}$
e		8	7	3	2	20	$J_{19} = J_{15} + J_{13} - J_{12}$
f		7	7	3	2	19	$J_{19} = J_{15}$
g		6	7	3	2	18	$J_{19} = J_{15} + J_{12} - J_{12}$
h		5	7	3	2	17	$J_{19} = J_{15} + J_{12}$

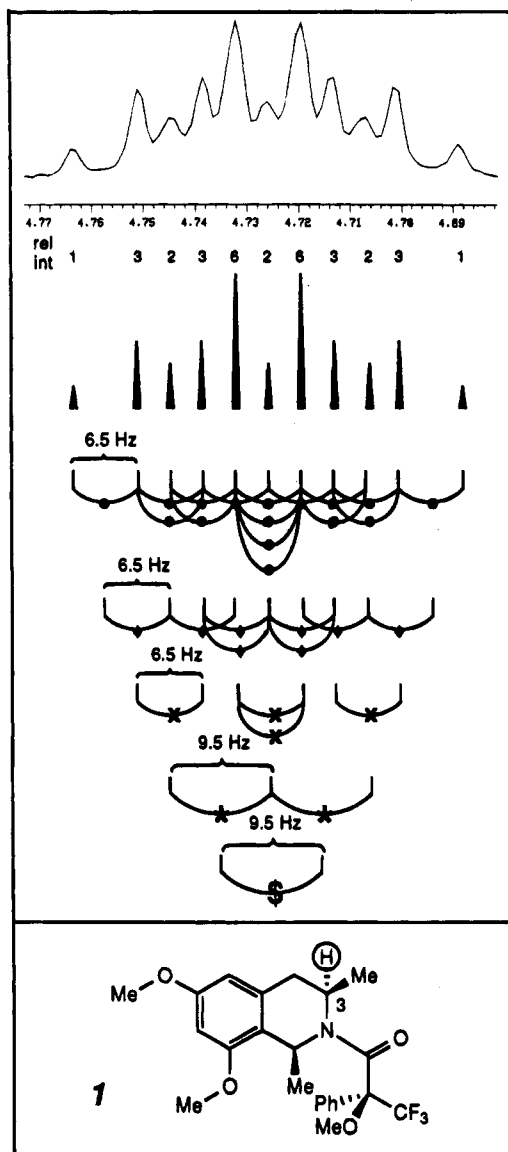
  

$\delta = 2.23$ , dddd,  $J = 15.5, 10.6, 5.1, 3.0$  Hz  
entry c

$\delta = 1.41$ , dddd,  $J = 12.3, 9.4, 7.4, 3.0$  Hz  
entry d

the ddd are identical so that the multiplets are all apparent doublets of triplets (6 lines), sometimes with additional simplification arising from additional special relationships [e.g., entries d (5 lines), h (4 lines), and l (3

Chart 3. Inverted Splitting Tree Analysis for the ddq (app tq) from H(3) in One Rotamer of the Mosher Amide 1



lines)]. Table 3 contains the cases where the two invariant coupling constants are only slightly different. The illustrated example, in which the central two lines of the ddd coincide and for which the largest  $J$  value is the sum of the two smaller  $J$ 's (i.e.,  $J_{x(15)} = J_{y(13)} + J_{z(12)}$  cf. entry c), is a commonly encountered one. This relationship and pattern (a seven-line 1:1:1:2:1:1:1 multiplet) are also seen in the example accompanying Table 4 (entry d). Table 5 illustrates the case where one of the invariant  $J$ 's is always significantly larger than the second ( $J_{y(13)} \gg J_{z(12)}$ ). The multiplet arising from the boxed proton in the example molecule corresponds to a situation intermediate between entries c and d and illustrates an important point. Namely, to find the best fit one must sometimes envision the continuum of multiplets that arise by sliding together the two halves of the pattern for entry a (as  $J_z$  decreases) within any one table. There often is not a perfect correlation between the multiplet under analysis and a specific table entry.

Tables 6–11 show doublet of doublet of doublet of doublets (dddd's) that increase in their complexity as the tables progress. Table 6 illustrates the case where three of the four  $J$ 's are equal, resulting in an apparent doublet

of quartets (i.e., app dq). This type of relationship is prevalent in rigid ring systems either where a geminal and two diaxial couplings give three approximately equivalent  $J$ 's and the fourth and smallest  $J$  arises from the gauche axial-equatorial arrangement of a pair of vicinal protons or, as is the case for the example of the boxed proton (cf. entry c), where a single large geminal coupling is accompanied by three approximately equivalent and small gauche couplings. The special relationship where the largest  $J$  is twice as large as any of the equivalent smallest  $J$ 's is present in the example of the circled proton (cf. entry f) and results in the greatly simplified six-line pattern. Table 7 shows multiplets that contain two pairs of identical  $J$ 's (i.e., app tt's). The example in Table 7 (cf. entry e) is commonly encountered in acyclic molecules where a methine proton is flanked by two methylene groups that each constitutes a pair of diastereotopic protons. Table 8 depicts dddd's in which the two  $J$ 's of intermediate magnitude are identical (i.e., app dtd's). Notice that the smallest  $J$  (1 Hz) in the example multiplet (cf. entry a) arises from four-bond W-coupling. Table 9 presents multiplets in which the two smallest  $J$ 's are identical in magnitude (i.e., app ddt's), although cases where the value of  $J_{z(17)}$  drops below  $J_{y(13)}$  are not shown. Another commonly encountered ddt arises from the methine of a terminal allyl group (i.e.,  $\text{CH}_2=\text{CHCH}_2\text{R}$ , not shown).

Tables 10 and 11 include representative cases of dddd's to which no universal special relationship applies (as is the case for Tables 6–9). Thus, for the first time among Tables 6–11 some of the entries show multiplets having the full complement of sixteen lines. The multiplets in Table 10 contain three and those in Table 11 contain two small  $J$ 's of nearly equal magnitude.

Recognize that there exist other possible combinations for the relative magnitudes of  $J$ 's within the family of dddd's than those shown in Tables 6–11. Recall that *all* permutations of  $J$  values for the simpler dd's and ddd's were encompassed by Tables 1 and 2–5, respectively. When in need, the reader is encouraged to extend the methods described here to those cases of  $J$  value combinations for dddd's not explicitly covered as well as to yet more complex multiplets like the ddddd's.

We conclude with one example of the latter. Chart 3 shows the multiplet arising from H(3) in the minor rotamer of the indicated Mosher amide.<sup>6f</sup> The multiplet was identified by the inverted splitting tree method as a ddq with  $J = 9.5, 9.5,$  and  $6.5$  by the sequence of steps outlined in Chart 3. This set of coupling constants requires that the molecule exists largely in the conformation having dihedral angles of  $\sim 150^\circ$  and  $30^\circ$  between H(3)/H(4a) and H(3)/H(4b), respectively. It should be noted that it was not possible to identify the two vicinal 9.5 Hz  $J$ 's from the benzylic methylene resonances due to significant overlap among those resonances for the amide rotamers, even at 500 MHz.

We have found the complementary approaches of visual pattern recognition (C) as well as the more systematic and analytical methods described in A and B to be effective and powerful tools. These approaches permit easy access to the rich, intrinsic information that is universally available via the simplest of NMR experiments.

**Acknowledgment.** This work was supported by the DHHS Grants GM 34492 and 39339. We acknowledge Mr. Zhixiong Ye for enunciating ideas that aided the development of the systematic analysis of line spacings and inverted splitting tree generation described here.